

# Optimisation of LT-GaN nucleation layer growth conditions for the improvement of electrical and optical parameters of GaN layers

MATEUSZ WOŚKO

Faculty of Microsystem Electronics and Photonic, Wrocław University of Science and Technology,  
Janiszewskiego 11/17, 50-372 Wrocław, Poland; mateusz.wosko@pwr.edu.pl

In this work we present the influence of low temperature gallium nitride (LT-GaN) nucleation layer deposition and recrystallization conditions on the electrical and optical properties of buffer and active layer of metal–semiconductor field-effect transistor (MESFET) structure. MESFET structures were used to investigate the properties of bulk materials that determine also the performance of many type GaN based devices, like light emitting diodes (LEDs), high electron mobility transistors (HEMTs) and metal–semiconductor–metal (MSM) detectors. The set of n-GaN/u-GaN/sapphire structures using different nucleation LT-GaN layers thickness and different annealing times was deposited using AIXTRON CCS epitaxial system. In contrast to typical procedure, the high resistive GaN buffer layer was not obtained by intentional Fe/Mg doping, but by specific adjustment of GaN nucleation conditions and recrystallization process parameters that introduce carbon atoms in epitaxial layers, that serve as donors. Generally, low pressure (below 200 mbar) in a reactor chamber, during initial stages of nucleation and recrystallization as well as HT-GaN epitaxy, promotes the growth of high resistive material. Obtained results show that annealing/recrystallization time of LT-GaN has a significant impact on the electrical and optical properties of GaN buffer layers. Longer annealing periods tend to promote crystallization of material with higher electron mobility and higher Si dopant incorporation/activation while maintaining high resistivity in u-GaN buffer area. It was shown that the dimensions of the GaN islands, that could be influenced by the duration of an annealing step of LT-GaN growth, have no impact on the HT-GaN buffer layer coalescence process and material resistivity, but influences mainly electrical properties of active n-GaN layer. Author suggests that the key parameters that are determining the buffer resistivity are the pressure and temperature during LT-GaN annealing and buffer layer coalescence. The influence of GaN island diameters, after LT-GaN annealing, on the u-GaN resistivity was not confirmed.

Keywords: GaN, nucleation, recrystallization, metalorganic chemical vapor deposition, nitrides, LED, MSM, MESFET devices.

## 1. Introduction

Al<sub>III</sub>-N materials are of great interest in optoelectronic and electronic devices because of their direct and wide band gap. Additionally, high electron saturation velocity of  $2.5 \times 10^7$  cm/s in AlGaN/GaN high electron mobility transistor (HEMT) channel, high breakdown field of 3 MV/cm and outstanding thermal stability of nitrides, make its

heterostructures competitive to the top SiC metal–semiconductor field-effect transistor (MESFET) devices. Although GaN light emitting diodes (LEDs), MESFETs and AlGaN/GaN HEMTs are commercially available, there is still much potential to improve devices performance mainly by improving the quality of thick buffer layers.

There are several factors that determine the applicability of AlGaN and GaN materials for devices. The principal requirement is the possibility to grow a high resistive GaN buffer layer. The second important requirement is its optical and electrical quality. There are other factors determining properties and usefulness of particular GaN buffer for device, however these two requirements are general and application independent.

The influence of low temperature nitride nucleation layer on the properties of subsequently grown high temperature GaN layers was extensively investigated over last two decades [1–5]. These works were focused mainly on the crystalline quality obtained by different sapphire substrate preparation and subsequent nucleation layer composition, thickness and growth conditions. So far there was limited information on the impact of initial stages of (Al, Ga)N epitaxy on the electrical properties of the field effect devices active structures. The increased interest in GaN based optoelectronic and microelectronic devices, especially in LEDs, MSMs, MESFETs and HEMTs, in the early years of 2000 encouraged to undertake research concerning crystallization of highly resistive buffer layers and the role of nucleation and initial stages of high temperature growth layer in formation of electrically isolating material. The comprehensive studies in this area are presented by several groups [6–11]. Although the formation mechanism of highly resistive undoped buffer GaN layers by adjustment of initial stages of GaN epitaxy is well known, there were no studies regarding the influence of the low temperature (LT) GaN growth parameters and its annealing conditions on the electrical properties of active layers, subsequently deposited on the buffer. This work shows that adjustment of the parameters of nucleation layer growth and annealing has a significant impact on the optical and electrical properties of GaN layers that are dedicated to optoelectronic and microelectronic devices such as metal–semiconductor–metal (MSM) photodetectors, HEMTs and MESFETs.

## 2. Experimental details

To study the influence of the buffer layer deposition and annealing parameters on the u-GaN buffer layer resistivity and subsequent active GaN layer electrical parameters, the MESFET structures (n-GaN/u-GaN/LT-GaN/sapphire) were grown by MOVPE technique using AIXTRON CCS system. Prior to material growth, C-plane sapphire substrate was thermally cleaned by 10 min in 1100°C. After that, the sapphire surface was NH<sub>3</sub> treated in 540°C for 3 min, and the LT-GaN nucleation layer (28 and 46 nm thick) was deposited. The nucleation layer was annealed during temperature ramp from 540 to 1045°C. The temperature increase time period was 180, 360 and 540 seconds. Highly resistive HT-GaN (high temperature GaN) buffer layer (1800 nm) was grown in 1045°C and 200 nm Si doped GaN was subsequently deposited on top of the structure. TMGa (trimethylgallium), NH<sub>3</sub> and 100 ppm mixture of SiH<sub>4</sub> in H<sub>2</sub> were used as pre-

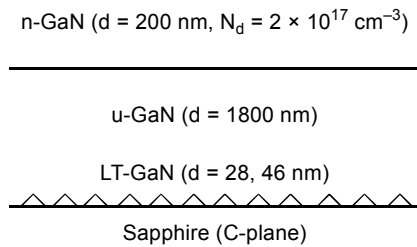


Fig. 1. The layer scheme of investigated n-GaN/u-GaN/LT-GaN structures.

cursors and dopant, respectively. GaN crystallization process was controlled *in situ* by 635 nm reflectometer. The layer scheme of investigated structures is presented in Fig. 1.

## 2.1. Growth studies of thin LT-GaN

Prior to relevant studies of the influence of LT-GaN annealing conditions on the properties of HT-GaN structure, the calibration procedure of LT-GaN growth was conducted. In order to determine the thickness of thin epitaxial layers (in the range of tens of nanometers), the new measurement procedure was proposed. In this method, the nucleation layer was ablated by 266 nm laser to form deep trenches in the epitaxial layer. Taking into account transparency of sapphire at 266 nm, the laser beam interacts only with deposited GaN material, remaining sapphire unaffected. The depth profiles of trenches were obtained by atomic force microscopy (AFM) technique and statistical procedure was applied to estimate the height coordinates of the GaN surface and sapphire surface in the trenches. The scanning electron microscopy (SEM) image of the LT-GaN surface with ablated trenches and its depth profile obtained by AFM method are presented in Fig. 2.

LT-GaN thickness values obtained by this method were correlated with the growth times and the *in situ* reflectance traces. It is worth to mention that the layer thickness

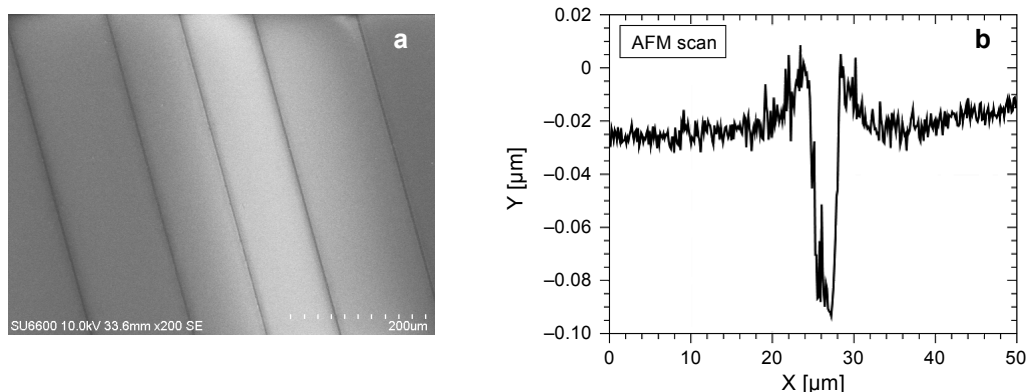


Fig. 2. SEM image of the LT-GaN layer surface (a) and AFM profile of the trench (b) after laser ablation.

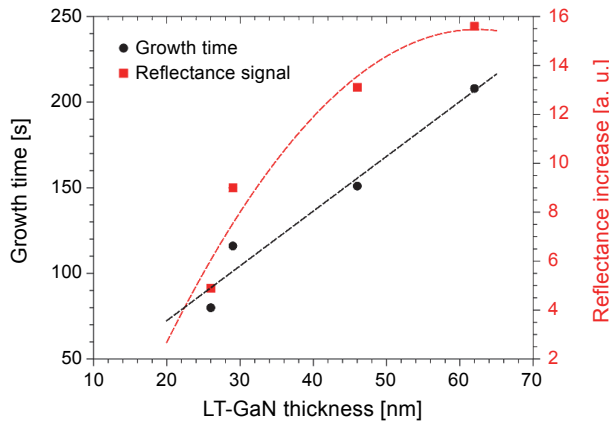


Fig. 3. Relations between LT-GaN thickness, reflectance increase value and reflectance increase time. Lines are a guide to the eye.

is not linearly correlated with TMGa dosing time. This is caused by the initial adsorption of precursors on the reactor wall and reduction of material crystallization efficiency on the substrate. Aforesaid conclusion is justified by the fact that part of samples was deposited after thermal cleaning of the reactor chamber and in that case, the growth of LT-GaN (monitored by a reflectometer) was delayed. Both the „true” growth time (the time at which the reflectance signal increases) and the reflectance value are correlated with the LT-GaN thicknesses. Obtained results are presented in Fig. 3. These calibration data were used for further study of n-GaN/u-GaN/LT-GaN/sapphire structures.

## 2.2. Growth and characterization of n-GaN/u-GaN/LT-GaN/sapphire

Deposited n-GaN/u-GaN/LT-GaN/sapphire structures were electrically characterized by the impedance spectroscopy method using mercury probe [12]. Capacitance spectra shown in Fig. 4a prove good isolation of all investigated buffer layers, however so-called buried conductive layer occurs, that is typical of the adopted method of highly resistive buffer layers fabrication. This is observed as a relatively small parasitic capacitance ( $\sim 40$  pF) at high depletion voltages. Based on  $C$ - $V$  (capacitance-voltage) measurements, the change of electron concentration in depleted region vs. bias voltage (Fig. 4b), as well as electron concentration profiles in the structures (Fig. 4c) were calculated. The strong influence of the LT-GaN annealing time on the efficiency of the Si incorporation/activation is clearly shown. The total electron density in n-GaN layer changes from  $1.5 \times 10^{12}$  to  $3.3 \times 10^{12} \text{ cm}^{-2}$  with the increase of annealing time from 180 to 540 s. Also the calculated electron mobility in n-GaN is strongly affected by LT-GaN layer annealing conditions (Fig. 5). For the 28 nm thick nucleation layer, the value of electron mobility and total electron concentration saturates for the annealing time of 360 s and is kept constant for 540 s. Whereas for the 46 nm thick layer, the electron mobility value saturates for the annealing period of 540 s. Another conclusion

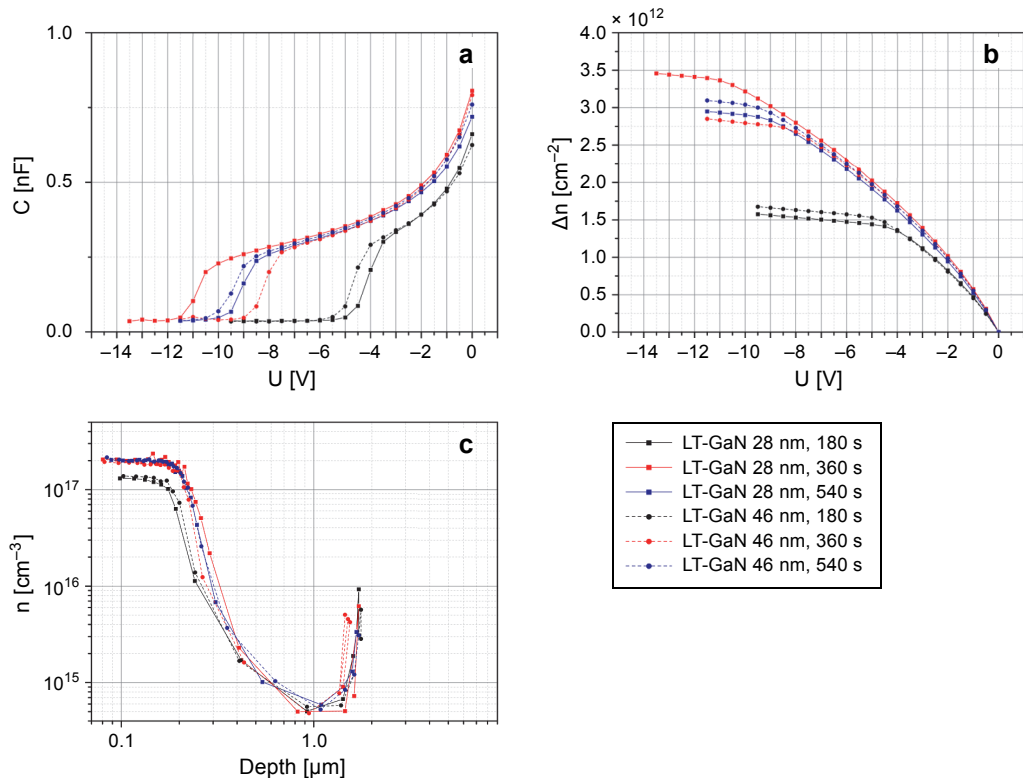


Fig. 4. The  $C$ - $V$  measurements results: the change of capacitance in depleted region (a) and electron concentration (b) vs. bias voltage. Calculated carrier concentration distribution in the n-GaN/u-GaN/LT-GaN structure (c).

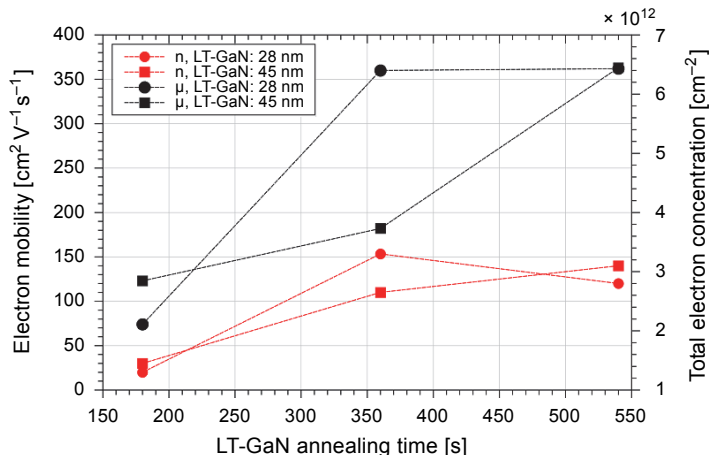


Fig. 5. Electron mobility and total electron concentration in n-GaN vs. LT-GaN annealing time. Lines are a guide to the eye.

can be formulated that despite of the LT-GaN layer thickness, the electrical properties of subsequently grown high temperature GaN layers are the same for the annealing time of 540 seconds.

The variation of the Si incorporation/activation efficiency in n-GaN layer with the annealing of LT-GaN nucleation layer suggests the influence of the annealing length on the crystalline structure of the material. To verify this assumption, the photoluminescence (PL) spectra of investigated n-GaN/u-GaN/LT-GaN/sapphire structures were measured at room temperature. The PL spectra in the range of band to band transition and yellow luminescence are presented in Fig. 6. It is clearly shown that regardless of the thickness of LT-GaN layer, the band to band GaN luminescence increases with the annealing time. The FWHM of this peak varies from 19 to 17 nm according to the annealing time. The total intensity of yellow luminescence increases with the annealing time of nucleation layer as well, however this increase is lower than the band to band luminescence. Moreover, it proves that longer LT-GaN annealing periods tend to pro-

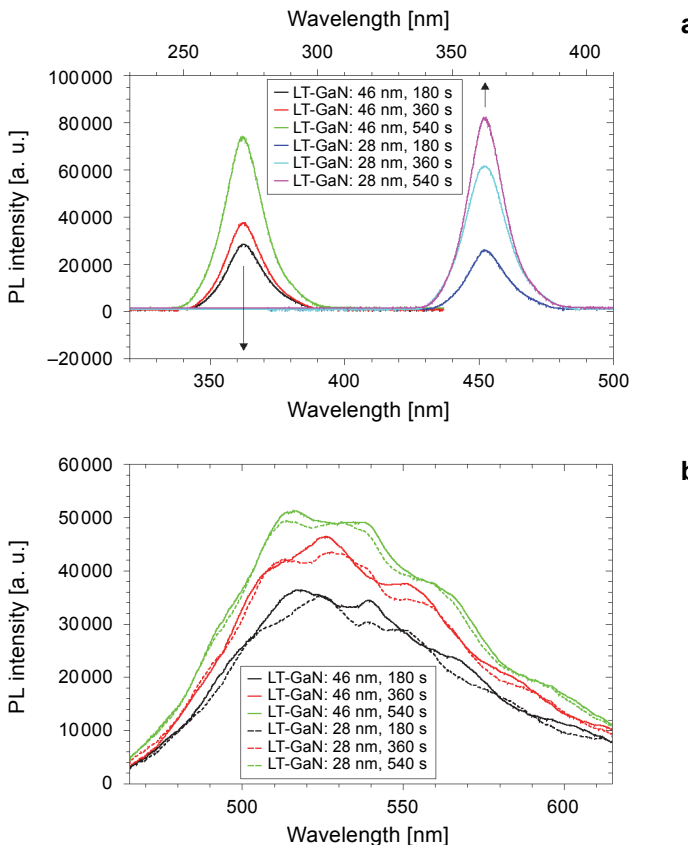


Fig. 6. PL spectra of n-GaN/u-GaN/LT-GaN structures of different thicknesses and different annealing times. Band to band (**a**) and yellow (**b**) luminescence.

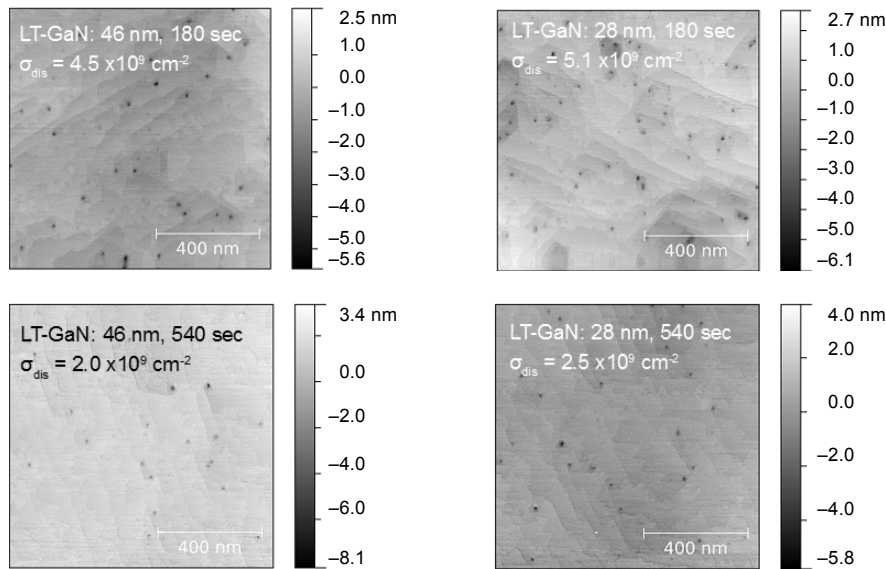


Fig. 7. Surface AFM scans of n-GaN/u-GaN/LT-GaN/sapphire structures with different LT-GaN thicknesses and annealing times.

mote HT-GaN growth of better crystalline quality. In order to determine the impact of early stages of nucleation on surface morphology, the AFM observations of investigated samples were done (Fig. 7). It is clearly shown that surface defects density (visible as black dots on the AFM scans) depends on LT-GaN thickness and annealing time. It decreases with extension of annealing period and thickening of the nucleation layer. The lowest defects density  $2.0 \times 10^9 \text{ cm}^{-2}$  is observed for 46 nm thick LT-GaN annealed by 540 s, whereas the highest  $5.1 \times 10^9 \text{ cm}^{-2}$  for 28 nm thick LT-GaN annealed by 180 s. This is consistent with previous reports on the impact of the annealed LT-GaN grain size on the crystalline quality and dislocation density in HT-GaN [8, 10].

The coalescence of bigger LT-GaN islands, during the annealing stage, takes more time, what is observed on the reflectance traces as an increase of the signal to the periodic oscillations (so-called recovery time), and results in better material quality. This is opposite to the mechanism of coalescence of smaller islands which promotes formation of threading dislocations in HT-GaN. The concentration of edge threading dislocation is closely correlated with the C atoms incorporation in the GaN what effectively enhances material resistivity. Furthermore, process parameters of early stages of GaN epitaxy on sapphire have a significant impact on material quality and electrical properties of epi-structures. Bigger LT-GaN islands result in better material quality, however smaller islands promote formation of highly resistive material, but with lower crystallographic quality and probably lower mobility due to stronger electron dispersion mechanism. From the point of view of devices applications this is a crucial problem. By adjusting the LT-GaN islands size, it is possible to grow low resistive material with high electron

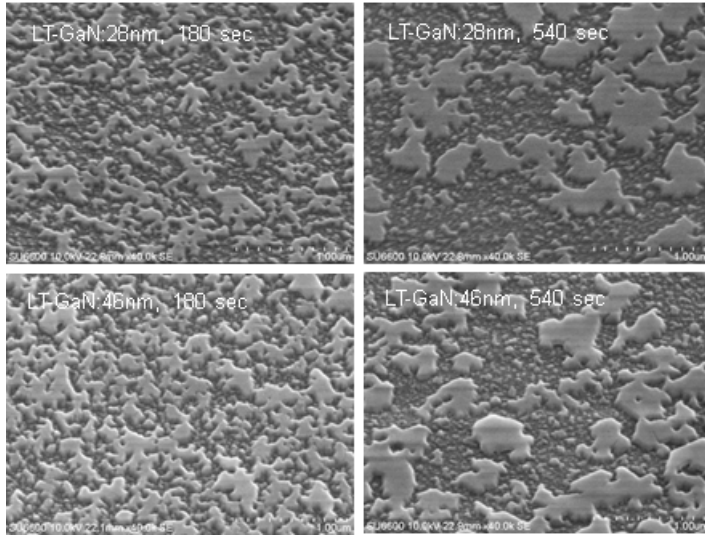


Fig. 8. SEM images of annealed LT-GaN nucleation layers of different layer thickness and annealing times.

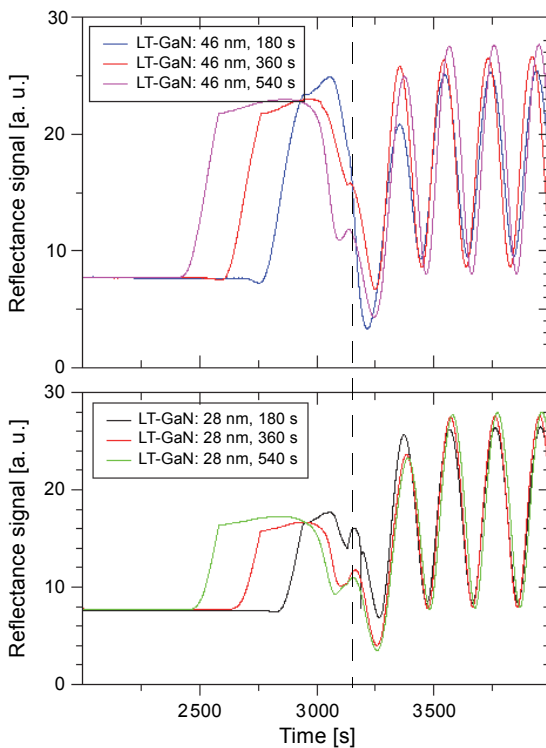


Fig. 9. Reflectance traces of nucleation LT-GaN layer growth, annealing and buffer HT-GaN layer coalescence. The beginning of the crystallization of HT-GaN is marked with a dashed line.

mobility or highly resistive material but also with low electron mobility. It is essential to find growth conditions that result in both good material resistivity and good material quality simultaneously.

To verify the correlation between electrical properties of HT-GaN layer and growth parameters of LT-GaN, the SEM measurements of annealed LT-GaN layers of different thickness were carried out. Obtained results (Fig. 8) show that annealing time has a strong impact on the size of the islands. However, differences in coalescence times of the layers with different grain sizes were not observed (Fig. 9). Moreover, changes in HT-GaN buffer resistivity were not distinguishable. It means that the LT-GaN nucleation layer island size is not the explicit parameter determining the resistivity of HT-GaN buffer layer and other process parameters must be considered as essential during the growth of highly resistive material. Observation of *in situ* reflectance traces proves a strong correlation between so-called “recovery time” (layer coalescence time) and GaN buffer resistivity.

### 3. Conclusions

The influence of the LT-GaN nucleation layer thickness and annealing time on the electrical and optical properties of n-GaN/u-GaN/LT-GaN/sapphire structures was investigated. It was observed that longer annealing/migration times of LT-GaN nucleation layers promote crystallization of optically and electrically better HT-GaN material – stronger band to band PL, higher Si incorporation/activation and higher electron mobility. Annealing time of LT-GaN nucleation layer does not affect the resistivity of undoped layer and the recovery time of reflectance signal during coalescence of buffer layer. Annealing times influence the diameter of GaN nucleation islands and surface defects density, however have no impact on the buffer resistivity.

*Acknowledgments* – This work was co-financed by the National Centre for Research and Development grants TECHMATSTRATEG No. 1/346922/4/NCBR/2017 and LIDER No. 027/533/L-5/13/NCBR/2014, the National Science Centre grant No. DEC-2015/19/B/ST7/02494, Wrocław University of Science and Technology statutory grants and by the Slovak-Polish International Cooperation Program. This work was accomplished thanks to the product indicators and result indicators achieved within the projects co-financed by the European Union within the framework of the European Regional Development Fund, through a grant from the Innovative Economy (POIG.01.01.02-00-008/08-05) and by the National Centre for Research and Development through the Applied Research Program Grant No. 178782.

### References

- [1] AMANO H., AKASAKI I., HIRAMATSU K., KOIDE N., SAWAKI N., *Effects of the buffer layer in metalorganic vapour phase epitaxy of GaN on sapphire substrate*, Thin Solid Films **163**, 1988, pp. 415–420, DOI: [10.1016/0040-6090\(88\)90458-0](https://doi.org/10.1016/0040-6090(88)90458-0).
- [2] WU X.H., FINI P., TARTA E.J., HEYING B., KELLER S., MISHRA U.K., DENBAARS S.P., SPECK J.S., *Dislocation generation in GaN heteroepitaxy*, Journal of Crystal Growth **189–190**, 1998, pp. 231–243, DOI: [10.1016/S0022-0248\(98\)00240-1](https://doi.org/10.1016/S0022-0248(98)00240-1).
- [3] WU X.H., KAPOLNEK D., TARTA E.J., HEYING B., KELLER S., KELLER B.P., MISHRA U.K., DENBAARS S.P., SPECK J.S., *Nucleation layer evolution in metal-organic chemical vapor deposition grown GaN*, Applied Physics Letters **68**(10), 1996, pp. 1371–1373, DOI: [10.1063/1.116083](https://doi.org/10.1063/1.116083).

- [4] AKASAKI I., AMANO H., KOIDE Y., HIRAMATSU K., SAWAKI N., *Effects of an buffer layer on crystallographic structure and on electrical and optical properties of GaN and  $Ga_{1-x}Al_xN$  ( $0 < x \leq 0.4$ ) films grown on sapphire substrate by MOVPE*, Journal of Crystal Growth **98**(1–2), 1989, pp. 209–219, DOI: [10.1016/0022-0248\(89\)90200-5](https://doi.org/10.1016/0022-0248(89)90200-5).
- [5] KAPOLNEK D., WU X.H., HEYING B., KELLER S., KELLER B.P., MISHRA U.K., DENBAARS S.P., SPECK J.S., *Structural evolution in epitaxial metalorganic chemical vapor deposition grown GaN films on sapphire*, Applied Physics Letters **67**(11), 1995, p. 1541, DOI: [10.1063/1.114486](https://doi.org/10.1063/1.114486).
- [6] CHEN J., ZHANG S., ZHANG B., ZHU J., FENG G., DUAN L., WANG Y., YANG H., ZHENG W., *Influence of growth pressure of a GaN buffer layer on the properties of MOCVD GaN*, Science in China Series E **46**(6), 2003, pp. 620–626, DOI: [10.1360/03ye0038](https://doi.org/10.1360/03ye0038).
- [7] WICKENDEN A.E., KOLESKE D.D., HENRY R.L., TWIGG M.E., FATEMI M., *Resistivity control in unintentionally doped GaN films grown by MOCVD*, Journal of Crystal Growth **260**(1–2), 2004, pp. 54–62, DOI: [10.1016/j.jcrysGro.2003.08.024](https://doi.org/10.1016/j.jcrysGro.2003.08.024).
- [8] HUBBARD S.M., ZHAO G., PAVLIDIS D., SUTTON W., CHO E., *High-resistivity GaN buffer templates and their optimization for GaN-based HFET's*, Journal of Crystal Growth **284**(3–4), 2005, pp. 297–305, DOI: [10.1016/j.jcrysGro.2005.06.022](https://doi.org/10.1016/j.jcrysGro.2005.06.022).
- [9] KOLESKE D.D., WICKENDEN A.E., HENRY R.L., TWIGG M.E., *Influence of MOVPE growth conditions on carbon and silicon concentrations in GaN*, Journal of Crystal Growth **242**(1–2), 2002, pp. 55–69, DOI: [10.1016/S0022-0248\(02\)01348-9](https://doi.org/10.1016/S0022-0248(02)01348-9).
- [10] GRZEGORCZYK A.P., MACHT L., HAGEMAN P.R., RUDZINSKI M., LARSEN P.K., *Resistivity control of unintentionally doped GaN films*, Physica Status Solidi C **2**(7), 2005, pp. 2113–2116, DOI: [10.1002/pssc.200461415](https://doi.org/10.1002/pssc.200461415).
- [11] MITA S., COLLAZO R., DALMAU R., SITAR Z., *Growth of highly resistive Ga-polar GaN by LP-MOVPE*, Physica Status Solidi C **4**(7), 2007, pp. 2260–2263, DOI: [10.1002/pssc.200674837](https://doi.org/10.1002/pssc.200674837).
- [12] PASZKIEWICZ B., WOSKO M., PASZKIEWICZ R., TLACZALA M., *Nondestructive method for evaluation of electrical parameters of AlGaN/GaN HEMT heterostructures*, Physica Status Solidi C **10**(3), 2013, pp. 490–493, DOI: [10.1002/pssc.201200709](https://doi.org/10.1002/pssc.201200709).

Received October 2, 2018  
in revised form January 13, 2019